# Impact of Graphs and Methodologies on Optical Access Networks Planning

Cristian Bermudez Serna[*], Anjali Sharma[†] and Carmen Mas-Machuca[*†]
[*]Chair of Communication Networks (LKN), Technical University of Munich (TUM), Germany
[†]Chair of Communication Networks, University of the Bundeswehr Munich (UniBW), Germany
cristian.bermudez-serna@tum.de, {anjali.sharma, cmas}@unibw.de

**Abstract**

Meeting the increasing capacity demands and availability requirements of modern optical access networks is crucial for network operators. Efficient planning tools are needed to evaluate new architectures over various areas before deciding on their adoption for a real deployment. This work shows the generalization capacity of Gabriel Graphs (GGs) for obtaining graphs with similar features from an input graph. The generated GGs allow to compare ILP formulations and a state-of-the-art Heuristic for planning Unprotected, Type A, and Type B Passive Optical Network (PON) architectures. The results show that the ILP requires, on average, 22% less fiber than the Heuristic. It is shown that the network's sparseness drives the fiber requirement, as planning PONs with the ILP in sparse GGs use, on average, 12% more fiber than over the original graph. It is also shown that the network operator would use a comparable amount of fiber in planning an unprotected PON with the state-of-the-art Heuristic and a protected PON using Type A or Type B with the ILP.

**Index Terms**

Optical Access Networks, Network Planning, Passive Optical Networks

## I. Introduction

Optical Access Networks (OANs) need to be upgraded due to the ever-increasing capacity required by end users and the significant increase and diversity of the connected end devices (WLAN routers, micro Base Stations, etc.). The optical fiber deployment starts from the Optical Line Terminal (OLT) at the Central Office (CO) towards the end users. Today, most densely populated areas have migrated from Fiber to the Cabinet (FTTCab) to Fiber to the Building (FTTB) and even Fiber to the Home/Flat (FTTH/F), depending on where the Optical Network Unit (ONU) is located. Given the high costs associated with the fiber roll-out, ONUs are connected to the OLT in a tree topology to minimize infrastructure costs. Passive power splitters are installed in the Remote Node (RN) locations to reduce operational costs, particularly power consumption, so the Optical Distribution Network (ODN) is entirely passive. This ODN is used by Passive Optical Networks (PONs) such as GPON (ITU-T G. 984) and XGPON (ITU-T G. 987), which use Time Division Multiplexing (TDM) techniques to allocate time slots for upstream and downstream data transmission as well as Wavelength Division Multiplexing (WDM) to transmit upstream and downstream on the same Fiber simultaneously. An example of the reference PON architecture is depicted in Figure 1a.

OAN operators, under the pressure of growing demand and competition, are considering new solutions to meet the requirements in the most economical way possible so they can maintain their benefits. To this end, evaluating the possible new solutions must be performed in a wide range of scenarios so that operators can decide whether to adopt a particular solution without running into unexpected overspending. Current studies evaluate the proposed solutions in particular areas or cities (e.g., Darmstadt [1], Valladolid [2], Cologne [3], Berlin, Helfenberg and Miesbach [4]). However, to generalize the performance metrics of the evaluated solutions, a much larger study has to be carried out. For this purpose, this paper evaluates the use of Gabriel Graph (GG) as a tool to generalize results, as GG can emulate various areas in terms of different characteristics. The number and length of street/road segments, density of intersections and ONUs, etc., can be varied, and the operator can better understand the most important criteria to be considered when deciding on adopting this particular solution. The solution considered in this study is the protection of the current unprotected PONs with two protection schemes proposed by the ITU-T [5].

This paper is structured as follows: Section II overviews the planning methodology and the state of the art. Section III is devoted to the generation of GG and identifies the parameters that can be tuned to generate a wide and useful set of graphs. Section IV introduces the different protection schemes that will be evaluated in Section V. The evaluation will focus on the total cost and the different cost categories. Finally, Section VI concludes the paper.

## II. Methodology and related works

An overview of the methodology used in OAN planning has been depicted in Figure 1b.

This work has been funded by the Federal Ministry of Education and Research in Germany (BMBF) under the projects AI-NET-ANTILLAS (Grant ID 16KIS1318) and FRONT-RUNNER (Grant ID 16KISR009).

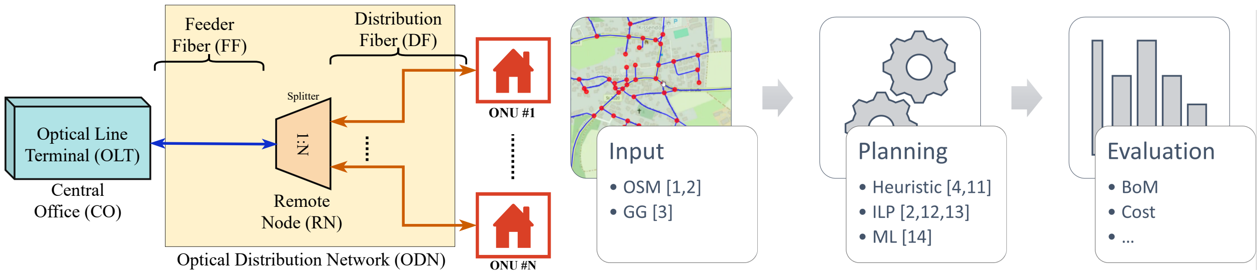


(a) Basic PON architecture. (b) Optical Access Network (OAN) planning methodology.

Fig. 1. Reference PON architecture and methodology overview.

**Input** When planning an OAN, information about the area and the distribution of users and any other end terminals (e.g., base stations) within the area is required. The information about the area also includes the surface, the street layout, the location of the CO, and the surface type of each street. This information can be obtained from open sources e.g.,Open Street Map (OSM) [6], which is gathered from public data and hence, it may be incomplete.

Although the use of a specific area is useful for operators when planning the network roll out, it is not suitable for evaluating new technologies, architectures or solutions. For this evaluation case, operators need to use graphs that emulate the generic street layout of different areas. One way of abstracting the street topology is to create a geometric model based on the average topology characteristics and reuse regular structures, e.g., the Triangular model (TM) [7]. However, it has been shown that neglecting the graph structure of the road topology leads to unpredictable over- and underestimation of the costs by up to 30% [8]. In this case, the results of strategic network planning cannot be used for decision making and the analysis is not reliable. Another way of abstracting the road topology is to create a graph-based abstraction. Maniadakis and Varoutas [9] propose the use of GG [10], which is applied in a small FTTB case study. This study compares the use of GG topologies with the most popular geometric models such as the Simplified Street Length model and the TM [7]. The study has shown that GG provides an accurate estimate of the real trenching costs that are the cost driver of OAN deployment. Based on these results, this study considers GG to emulate different street layouts.

A critical aspect in OAN planning are the number and location of the end points that have to be connected (e.g., houses and flats in FTTH/F, buildings in FTTB, and Base stations). The information on some end points are publicly available (e.g., buildings at OSM [6]). However, the location and number of end points are also parameters that need to change in order to generalise the performed evaluation and comparisons mentioned above.

**Planning** The planning of OANs consists of finding the location of the RNs as well as the fiber layout to interconnect the CO to the given end points (ONUs). The objective of most of the proposed solutions is to minimize the cost or the required infrastructure. Some works use heuristics technique based on K-means clustering to group end-points according to the splitting ratio, aiming to minimize the total required fibers [4], [11]. It is important to stress that in order to obtain reliable results, the clustering should use the street/graph layout distance instead of the Euclidean distance. Despite the long computational times, optimization techniques (e.g., ILP) have been proposed to find the optimal solution [2], [12], [13]. To reduce the computation time, Machine Learning techniques have been suggested [14].

**Evaluation** The result of the OAN planning is usually given as a Bill of Material (BoM), which consists of the number and location of the different RNs as well as the required fibers and their layout. However, other metrics such as cost, cost per delivered *bps*, power consumption, and availability are also used for the evaluation [4].

## III. Gabriel Graphs

### A. Gabriel Graph Definition

Fig. 2a presents conceptually a GG. As depicted in Fig. 2b, in GGs, for all adjacent nodes, if a circumference is drawn having the two nodes circumscribed, the circumference should not enclose any other node of the graph. Eq. 1 defines the empty circle property of GGs. Consider the graph $G$ composed of the set of nodes $N$ and links $L$. $G$ is said to be a GG if the squared link Euclidean distance $d^2_{i,j}$ between the nodes $i$ and $j$ is less that the sum of squared link Euclidean distances $d^2_{i,k}$ and $d^2_{j,k}$ from nodes $i$ and $j$ to any other node $k$ in $G$.

$$d^2_{i,j} < d^2_{i,k} + d^2_{j,k}, \forall k \in G, k \neq i, k \neq j \tag{1}$$

### B. Gabriel Graph Generation

Given a set of nodes $N$, a GG can be generated by iterating over all three-node sets and applying Eq. 1. If the inequality is satisfied, a link is added. Otherwise, the next three-node set is evaluated. Generating the graph by applying Eq. 1 has $O(n^3)$ complexity, which may be computationally prohibitive for large sets of nodes.

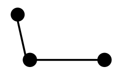

(a) Sample GG.

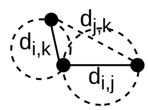


(b) Sample GG verification.

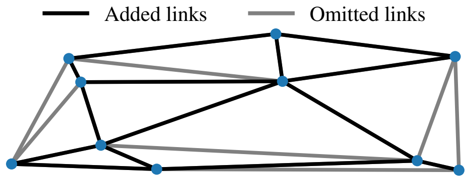


(c) Delaunay Triangulation $G_{DT}$.

Fig. 2. Fig. 2a depicts conceptually a GG. Fig. 2b depicts the empty circle property of GGs. The sample graph is a GG since only the adjacent nodes are within the circumferences. Fig. 2c Delaunay Triangulation $G_{DT}$ for ten random nodes. Links added and omitted from $G_{DT}$ are depicted with black and gray colors. The Gabriel Graph $G_{GG}$ consists only of the black links.

**Algorithm 1** Gabriel Graph Generation.

**Require:** Set of nodes $N$, optional target links number $l_T = 0$
**Ensure:** Gabriel Graph $G_{GG}$

1: $G_{GG} \leftarrow Graph\_Only\_Nodes(N)$
2: $G_{DT} \leftarrow Delaunay\_Triangulation(N)$
3: **for** Link $l_i$ in $G_{DT}$ **do**
4: $\quad G_{GG}.add\_link(l_i)$
5: $\quad$ **for** Node $n_j$ in $G_{DT}$ **do**
6: $\quad\quad$ **if** $l_i.is\_in\_circumcircle(n_j)$ **then**
7: $\quad\quad\quad G_{GG}.delete\_link(l_i)$
8: $\quad\quad\quad$ **break**
9: **while** $l_T > 0$ **and** $G_{GG}.get\_num\_links() > l_T$ **do**
10: $\quad l_d \leftarrow G_{GG}.delete\_random\_link()$
11: $\quad$ **if** **not** $G_{GG}.is\_connected()$ **then**
12: $\quad\quad G_{GG}.add\_link(l_d)$
13: **return** $G_{GG}$

Alg. 1 describes an alternative for efficiently generating a GG by leveraging the Delaunay Triangulation (DT). A DT divides the space into a set of triangles, where no other node lies within the circumcircle of any triangle. In lines 1-2, given $N$ nodes and an optional target links number $l_t$, a node-only GG $G_{GG}$ and a DT $G_{DT}$ are generated. $G_{DT}$ can be generated with a complexity $O(n\,log\,n)$. By definition, $G_{GG}$ is a subgraph of $G_{DT}$, i.e., $G_{GG} \subseteq G_{DT}$. Hence, $G_{GG}$ can be obtained by adding the links with empty circumcircles from $G_{DT}$, as described in lines 3-8. By definition, $G_{DT}$ is a planar graph, which implies that the number of links $l = |L|$ in $G_{DT}$ is upper-bounded by the number of links in the maximum connected planar graph generated with the set of nodes $N$ given by $l \leq 3n - 6$. Lines 3-8 iterate $l$ times, each time checking $n - 2$ nodes. Hence, the overall complexity for generating $G_{GG}$ by adding links from $G_{DT}$ is upper-bounded by $O(n\,log\,n + 3n^2)$. Optionally, lines 9-12 randomly remove links from $G_{GG}$ without creating a disconnected graph, as depending on the application, it may be desirable to have a targeted links number in $G_{GG}$. Line 13 returns $G_{GG}$. Fig. 2c shows the output of Alg. 1 for ten random nodes without randomly removing links.

## IV. Planning

In Section III, GGs and the algorithm for their generation were introduced. GGs are used to generalize the street layout of a target city. The PON planning tool uses the GGs as input to design the network while minimizing the total fiber length. This work focuses on the Unprotected and ITU-T Type A and Type B PON architectures shown in Figs. 3a-3c, respectively, and presents Integer Linear Programming (ILP) formulations for their planning. Moreover, a state-of-the-art Heuristic [4] for planning the Unprotected, Type A, and Type B PON architectures is also implemented and used to benchmark the ILP formulation.

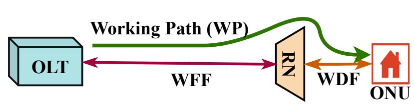


(a) Unprotected.

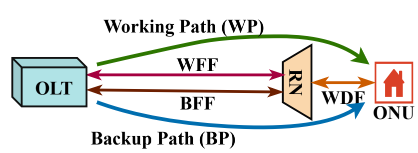


(b) Type A.

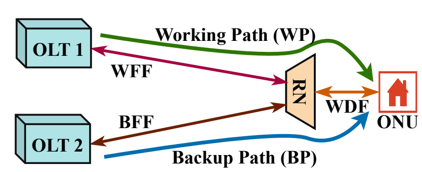


(c) Type B.

Fig. 3. PON architectures for Unprotected, Type A, and Type B, with Working Feeder Fiber (WFF), Working Distribution Fiber (WDF), Backup Feeder Fiber (BFF), Working Path (WP), and Backup Path (BP).

TABLE I
Variables and constants of ILP formulations for Unprotected and ITU-T Type A-B PON architectures in Eqns. 2-7.

| Inputs | |
|---|---|
| $X$ | Set of RNs $\{RN_1, ..., RN_n\}$. |
| $Y$ | Set of ONUs $\{ONU_1, ..., ONU_m\}$. |
| $O_i$ | Location of $OLT_i \in \{OLT_1, OLT_2\}$. |
| $a_{i,j}$ | Distance between nodes $i, j$. |
| $b_{i,j}$ | Backup distance between nodes $i, j$, link disjoint to $a_{i,j}$. |

| Inputs | |
|---|---|
| $N_{max}$ | Maximum number of splitters in a RN. |
| $SR$ | Splitters' splitting ratio. |
| **Variables** | |
| $n_i$ | Integer variable in $[0, N_{max}]$. Number of splitters in $RN_i$. |
| $x_{i,j}$ | Binary variable. 1 if $ONU_j$ is assigned to $RN_i$, else 0. |

### A. Unprotected ILP

The Unprotected PON architecture in Fig. 3a has no recovery mechanism against Feeder Fiber (FF) or Distribution Fiber (DF) failures, affecting the end-user if either of the fibers fails. The Unprotected ILP formulation in Eqn. 2 minimizes the total fiber length, consisting of the WFF between the OLT and all RNs, and the WDF between the RNs and their ONUs. The parameters and variables are summarized in Tbl. I. The constraints are enumerated in Eqns. 3-5.

**Unprotected fiber length minimization objective:**

$$min\left(\sum_{i\in X}\left[a_{i,O_1}\cdot n_i+\sum_{j\in Y}[a_{i,j}\cdot x_{i,j}]\right]\right) \tag{2}$$

**Single assignment constraint:** One $ONU_j$ can be assigned to only one $RN_i$.

$$\sum_{i\in X} x_{i,j}=1,\forall j\in Y \tag{3}$$

**Active RN constraint:** $RN_i$ can serve $ONU_j$, only if it has been setup and being used.

$$x_{i,j}\leq n_i,\forall i\in X,\forall j\in Y \tag{4}$$

**Splitting ratio constraint:** The number of ONUs connected to a $RN_i$ can not exceed the aggregated splitting ratio of the collocated splitters.

$$\sum_{j\in Y} x_{i,j}\leq SR\cdot n_i,\forall i\in X \tag{5}$$

### B. Type A ILP

Failure of FF has a higher impact than the DF as it affects all the ONUs connected to that FF and hence, it is the first component to be protected. Type A PON architecture in Fig 3b mitigates the connectivity loss due to a WFF failure by providing a BFF between OLT and RN. Switching from a failed WFF to a BFF is done using an optical switch. The Type A ILP formulation in Eqn. 6 minimizes the total fiber length, consisting of the WFF and the BFF between the OLT and all RNs, and the WDF between the RNs and their ONUs. The parameters and variables are summarized in Tbl. I. The constraints are enumerated in Eqns. 3-5.

**Type A fiber length minimization objective:**

$$min\left(\sum_{i\in X}\left[(a_{i,O_1}+b_{i,O_1})\cdot n_i+\sum_{j\in Y}[a_{i,j}\cdot x_{i,j}]\right]\right) \tag{6}$$

**Type B fiber length minimization objective:**

$$min\left(\sum_{i\in X}\left[(a_{i,O_1}+b_{i,O_2})\cdot n_i+\sum_{j\in Y}[a_{i,j}\cdot x_{i,j}]\right]\right) \tag{7}$$

**Algorithm 2** Heuristic for PON Planning [4].

**Require:** $G_{GG}$, Protection Type $P$, Splitting ratio $SR$, Set of ONUs $Y$, Distance matrices $a_{i,j}$, $b_{i,j}$
**Ensure:** Planned PON for $G_{GG}$ with Total Fiber
1: $G_{GG}^{P} \leftarrow GG\_preprocess\_(G_{GG},P)$
2: $G_{GG}^{ONU} \leftarrow GG\_ONU\_(G_{GG}^{P},Y)$
3: $G_{GG}^{CL} \leftarrow GG\_Clustering\_(G_{GG}^{ONU},SR)$
4: $G_{PL} \leftarrow RN\_Assignment\_(G_{GG}^{CL})$
5: $G_{PL}^{pr}$, Total Fiber$\leftarrow G_postprocess_(G_{PL},P,a_{i,j},b_{i,j})$
6: **return** $G_{PL}^{pr}$, Total Fiber

### C. Type B ILP

To prevent having the OLT as a single point of failure, Type B PON architecture in Fig. 3c mitigates the connectivity loss due to a failure of the OLT or WFF. It has BFF connecting the RN with a secondary OLT, placed sufficiently far from the primary OLT. Type B ILP formulation in Eqn. 7 minimizes the total fiber length, consisting of the WFF and the BFF between the primary and secondary OLTs, respectively and all RNs, and the WDF between the RNs and their ONUs. The parameters and variables are summarized in Tbl. I. The constraints are enumerated in Eqns. 3-5.

### D. Heuristic

The state-of-the-art Heuristic [4] in Alg. 2 starts with the graph $G_{GG}$, the protection type $P$, the splitting ratio $SR$, the set of ONUs and the distance matrices $a_{i,j}$ and $b_{i,j}$ of Tbl. I as inputs. In line 1, the pre-processing function $GG\_preprocess\_()$ removes the nodes with node degree one from $G_{GG}$ returning $G_{GG}^{P}$. In line 2, the function $GG\_ONU\_()$ uniformly distributes the set of ONUs $Y$ over all the links in $G_{GG}^{P}$ returning the graph $G_{GG}^{ONU}$. In line 3, the function $GG\_Clustering\_()$ divides the graph $G_{GG}^{ONU}$ into $K$ clusters using the K-means clustering algorithm and returns the graph $G_{GG}^{CL}$. $K$ is the ceiling value when the number of ONUs is divided by the $SR$. In line 4, for each cluster in the graph $G_{GG}^{CL}$, the function $RN\_Assignment\_()$ selects the RN closest to the cluster centroid and assigns all the ONUs in the cluster to it. Once the assignment process finishes, the function $RN\_Assignment\_()$ returns the planned graph $G_{PL}$. In line 5, the function $G\_postprocess\_()$ is performed, where $G_{PL}$ with $a_{i,j}$ and $b_{i,j}$ are used to calculate the length of the WFF, WDF, and BFF, according to protection type $P$. $P$ can be 0, A, and B for Unprotected, Type A, and Type B, respectively. $G\_postprocess\_()$ returns the planned network and the total fiber length.

## V. Evaluation

### A. Measurement Methodology

A graph covering an area of 2x2 $km^2$ of Chennai city with 881 links and 579 nodes is selected to perform the evaluations. The nodes with node-degree one are removed from the Chennai graph to obtain a bi-connected graph, where link disjoint paths between any pair of nodes can be found. After removing the links, the ChennaiNL graph with N=396 nodes and L=704 links is obtained. The Chennai graph and the GG generation described in Alg. 1 are used to obtain five samples for each of the following scenarios: *i)* GGNL having the same number of nodes and links as ChennaiNL, *ii)* GGN20L having 20% more links, i.e., 845 links, than ChennaiNL, *iii)* GG20NL having 20% more nodes, i.e., 475 nodes, than ChennaiNL, and *iv)* GG20N20L having 20% more nodes and links, i.e., 475 nodes and 845 links, than ChennaiNL. The ChennaiNL graph and the five generated graphs for GGNL, GGN20L, GG20NL and GG20N20L are used as input for the ILP and the Heuristic implementations of Unprotected, Type A and Type B PON architectures. In unprotected, Type A and Type B, the OLT is placed at the node with the highest closeness centrality. In Type B, the secondary OLT is placed at the node with the highest closeness centrality, which is at least 500 m away from the primary OLT. ONUs are uniformly distributed over the links of the graph and their number is kept constant at 1500 across all evaluations. As summarized in Figs. 4a-4d and Tbl. II, the metric selected for comparison is the total fiber length, comprising the WFF, WDF lengths, and when applicable, the BFF length.

### B. Gabriel Graphs Generalization Capacity

This evaluation investigates the GGs generalization capacity by comparing the results obtained in the input graph against those from the generated GGs. Fig. 4a and the GGNL row of Tbl. II present the total fiber results of the ILP and Heuristic implementations of the PON architectures for the ChennaiNL graph and the five GGNL graphs. As depicted, there is a subtle difference between the results of the ILP and Heuristic implementations for all schemes, where the total fiber length for ChennaiNL, in the worst case, is about 5% longer than for GGNL graphs. The results show that GGs obtained using Alg. 1 can generalize the features of the input graph with a small error margin. The discrepancy between the fiber lengths can be attributed to the fact that the street layout in the GGNL graphs does not entirely resemble the grid layout of ChennaiNL. As GGNL graphs are derived from a triangulation, triangles are predominantly found than squares, as is the case for ChennaiNL. The difference between ChennaiNL and the GGNL graphs may be alleviated by replacing the link removal policy in line 10 of Alg. 1 by other breaking triangles into a grid-like structure.

### C. ILP and Heuristic Comparison

As reported in Figs. 4a-4d, the ILP formulation uses less fiber than the Heuristic in each PON architecture. Focusing on the results for the ILP formulation and the Heuristic using the GGNL graphs in Fig. 4a and the GGNL row of Tbl. II, the ILP uses 24%, 21% and 21% less fiber for unprotected, Type A and Type B, respectively. Remarkably, an operator would use a comparable amount of fiber in planning an unprotected PON with the Heuristic and planning a protected PON using Type A or Type B with the ILP formulation.

TABLE II
Total length for Chennai and the GGs using the ILP and Heuristic implementations for Unprotected, Type A and Type B. The values for the GG are averaged over five samples.

| | **Unprotected [km]** | | **Type A [km]** | | **Type B [km]** | |
|---|---|---|---|---|---|---|
| | **ILP** | **Heu** | **ILP** | **Heu** | **ILP** | **Heu** |
| **ChennaiNL** | 208.1 | 274.6 | 288.1 | 362.3 | 282.9 | 356.7 |
| **GGNL** | 197.5 | 259.9 | 274.0 | 346.4 | 273.6 | 345.3 |
| **GGN20L** | 195.2 | 250.7 | 265.8 | 327.9 | 267.9 | 328.8 |
| **GG20NL** | 217.5 | 324.2 | 317.8 | 443.3 | 309.9 | 433.7 |
| **GG20N20L** | 201.3 | 268.4 | 280.1 | 355.6 | 278.6 | 353.6 |

### D. Unprotected, Type A, Type B Comparison

As reported in Figs. 4a-4d, the unprotected PON architecture, as expected, requires less fiber than Type A and Type B since no backup fibers are considered. Type A and Type B protection schemes require comparable fiber lengths. However, there is a slight fiber length reduction in favor of Type B, which can be seen in Fig. 4a and the GGNL row of Tbl. II for the GGNL graphs, where Type B requires 0.2% and 0.3% less fiber than Type A for the ILP and the Heuristic, respectively. The slight improvement of Type B over Type A protection scheme is attributed to the placement freedom of the secondary OLT. Having different locations for the primary and secondary OLTs in strategical central nodes of the network eases finding link disjoint paths for the BFFs and minimizes their distances. In comparison, Type A requires two link disjoint paths between the same source and destination, which complicates finding BFFs and negatively impacts their length.

### E. GGNL, GGN20L, GG20NL and GG20N20L Comparison

Figs. 4a-4d present the fiber length results for the ILP and the Heuristic for unprotected, Type A and Type B over the set of graphs for GGNL, GGN20L, GG20NL and GG20N20L. Comparing Figs. 4a with 4d and GGNL and GG20N20L rows of Tbl. II show that increasing the number of nodes and links by 20% results in a small increase of about 2% for the fiber length of the ILP for unprotected, Type A, and Type B. The small increase can be attributed to the proportional increase in the resources of the GG20N20L graphs, i.e., nodes and links, while keeping constant the area of the city and the ONUs number.

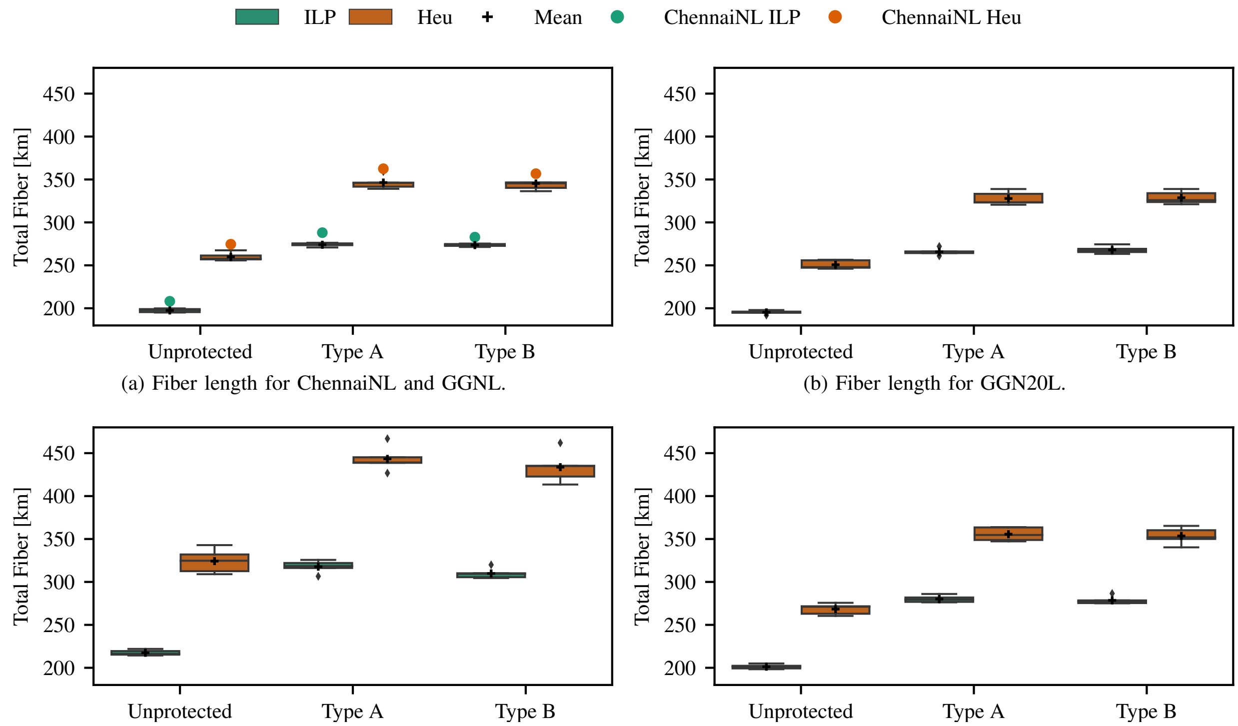


(a) Fiber length for ChennaiNL and GGNL.

(b) Fiber length for GGN20L.

(c) Fiber length for GG20NL.

(d) Fiber length for GG20N20L.

Fig. 4. Figs. 4a-4d present the fiber length results for the ILP and the Heuristic for unprotected, Type A and Type B over the ChennaiNL graph and the set of graphs for GGNL, GGN20L, GG20NL and GG20N20L with 1500 ONUs uniformly distributed over the links.

Comparing Figs. 4a with 4b and the GGNL and GGN20L rows of Tbl. II show that increasing the number of links by 20%, results in a small decrease of 1% , 3% and 2% for the fiber length of the ILP for unprotected, Type A, and Type B. The decrease in the fiber length can be attributed to the increased number of links that the ILP has disposition when selecting the shortest paths. Comparing Figs. 4a with 4c and the GGNL and GG20NL rows of Tbl. II show that increasing the number of nodes by 20%, results in a large increase of 9% , 14% and 12% for the fiber length of the ILP for unprotected, Type A, and Type B. The large increase in the fiber length can be attributed to the sparse nature graphs GG20NL, since the same number of links need to connect an increased number of nodes, resulting in longer links being available for the ILP when selecting the shortest paths.

## VI. Conclusions

This paper presents an approach to evaluate planning tools for OAN using an algorithm based on GGs that generalizes the features of an input city graph and produces graphs with a parameterized number of nodes and links. The Unprotected, Type A and Type B PON architectures are selected as use cases, for which network planning tools based on an ILP formulations and a state-of-the-art heuristic are provided. The city of Chennai is selected for evaluation and the total fiber length required for the deployment is used as a metric. The results show that the proposed GG algorithm can effectively generalize the input city graph and produce results differing in the worst case in 5% compared to the results of the original city graph. The results suggest that Type B is a better approach than Type A when planning a protected PON, in case the OLTs are placed in strategic nodes with high closeness centrality. Type B offers improved reliability because the secondary OLT being placed in a different location, which eases finding link disjoint paths and subtly reduces their lengths. The evaluation of the graph with 20% more nodes than the original shows that the sparseness of the network is the primary driver in the increase in fiber length when planning a network. Hence, a strategic link addition is an efficient mechanism to reduce the fiber length when planning a PON. Lastly, the results highlight the importance of using exact methods over heuristics, as an operator would use a comparable amount of fiber in planning an Unprotected PON with the state-of-the-art Heuristic and a protected PON using Type A or Type B with the ILP formulation. There is a future scope in refining the GG generation algorithm to close the gap between the results of the input graph and the generated graphs, as well as evaluating other protection schemes such as Type C.

## References

[1] M. Rahman, C. Mas-Machuca, K. Grobe, and W. Kellerer, "Advantages of joint access network planning in dense populated areas," in *2014 19th European Conf. on Networks and Optical Communications - (NOC)*, 2014, pp. 67–73.

[2] C. Anzola-Rojas, R. J. Durán Barroso, I. de Miguel, N. Merayo, J. C. Aguado, P. Fernández, R. M. Lorenzo, and E. J. Abril, "Resilient planning for multi-access edge computing in sparsely populated areas," in *18th Int. Conf. on the Design of Reliable Communication Networks (DRCN)*, 2022.
[3] M. Bongard, K. Grunert, and S. Aleksic, "Techno-economic analysis of deployment options for converged 5g wireless-optical access networks," in *2020 43rd Int. Convention on Information, Communication and Electronic Technology (MIPRO)*, 2020, pp. 401–406.
[4] A. Shahid and C. Mas-Machuca, "Dimensioning and assessment of protected converged optical access networks," *IEEE Communications Magazine*, vol. 55, no. 8, pp. 179–187, 2017.
[5] ITU-T Series G: Transmission systems and media, Digital systems and networks, "Passive Optical Network protection and considerations," https://www.itu.int/rec/T-REC-G.Sup51-201706-I, 2017.
[6] OpenStreetMap contributors, "Planet dump retrieved from https://planet.osm.org ," https://www.openstreetmap.org , 2017.
[7] D. Gardan, A. Zaganiaris, A. Madani, R. Madigou, and D. Machon, "Techno-economics of advanced optical subscriber networks," in *Global Telecom. Conf. and Exhibition'Communications Technology for the 1990s and Beyond'(GLOBECOM), 1989. IEEE.* IEEE, 1989, pp. 1335–1339.
[8] A. Mitcsenkov, M. Kantor, K. Casier, B. Lannoo, K. Wajda, J. Chen, and L. Wosinska, "Geometric versus geographic models for the estimation of an FTTH deployment," *Telecommunication Systems*, vol. 54, no. 2, pp. 113–127, 2013.
[9] D. Maniadakis and D. Varoutas, "Incorporating Gabriel graph model for FTTx dimensioning," *Photonic Network Communications*, vol. 29, no. 2, pp. 214–226, 2015.
[10] K. R. Gabriel and R. R. Sokal, "A new statistical approach to geographic variation analysis," *Systematic zoology*, vol. 18, no. 3, pp. 259–278, 1969.
[11] C. Mas-Machuca, L. Wosinska, and J. Chen, "Assessment methodology of protection schemes for next generation optical access networks," *Optical Fiber Technology*, vol. 26, pp. 82–93, 2015, next Generation Access Networks. [Online]. Available: https://www.sciencedirect.com/science/article/pii/S1068520015000991
[12] F. Verdaguer, C. Mas-Machuca, and K. Grobe, "Performance Analysis of Wavelength-Routed WDM-PON in Mobile x-Haul," *Conf. of Telecommunication, Media and Internet Techno-Economic Proceedings*, 2015.
[13] D. B. Shmoys, E. Tardos, and K. Aardal, "Approximation algorithms for facility location problems (extended abstract)," in *Proceedings of the Twenty-Ninth Annual ACM Symposium on Theory of Computing*, ser. STOC '97. New York, NY, USA: Association for Computing Machinery, 1997, p. 265–274. [Online]. Available: https://doi.org/10.1145/258533.258600
[14] A. K. Nayak, D. Tiwari, and S. Pattanayak, "Intellifiber: Optical network optimization through machine learning algorithms," in *2023 14th Int. Conf. on Computing Communication and Networking Technologies (ICCCNT)*, 2023, pp. 1–9.